THEORETICAL ANALYSIS OF THE POTTER HORN-REFLECTOR ANTENNA FOR SUBMILLIMETRE-WAVE APPLICATIONS

G. YASSIN, S. WITHINGTON, P. KITTARA AND K. G. ISAAK
Department of Physics, University of Cambridge,
Madingley Road, Cambridge CB3 OHE, UK

ABSTRACT We present a new horn-reflector feed design for SIS mixers. The antenna comprises an offset parabolic reflector fed by a Picket-Potter horn. The horn is easy to machine, and yet still preserves the desirable electrical properties of a corrugated horn, namely low cross polarisation and low sidelobe level, albeit over a reduced bandwidth. We calculate the aperture field distribution and the scattering matrix of the horn using the modal matching method and provide design curves which show the dependence of the beamwidth and the cross polarisation level on the antenna design parameters.

INTRODUCTION

The horn-reflector antenna is an offset parabolic reflector fed by a metallic horn. This arrangement is used to increase the aperture efficiency of the antenna without using lenses. When fed by a corrugated horn, the antenna has the additional advantage of low cross polarisation and sidelobe level. In a previous publication (Withington *et. al*, 1996) we demonstrated that this antenna is suitable for SIS mixer optics, guaranteeing efficient coupling between the telescope and the SIS detector over a large bandwidth. Such good performance, however, can only be achieved if a high rate of corrugations is maintained deep in the throat of the horn in order to prevent the excitation of higher order modes. Clearly, machining of corrugations in the horn throat at submillimetre-wavelengths is difficult, and the practical realisation of this unique design becomes very awkward at THz frequencies, and very expensive and time consuming for imaging arrays.

In this paper we present a new horn-reflector antenna design which employs a Picket-Potter horn, which is essentially a smooth-wall conical horn, with a single step at the throat. We show that this horn, clearly much easier to manufacture than the corrugated horn, has comparable electrical characteristics over a 15% fractional bandwidth.
We have developed software which allows us to predict accurately the performance of the Potter horn-reflector antenna. This is done by calculating the scattering matrix and the aperture field distribution of the horn using a modal matching technique, followed by the conformal mapping of the horn fields onto

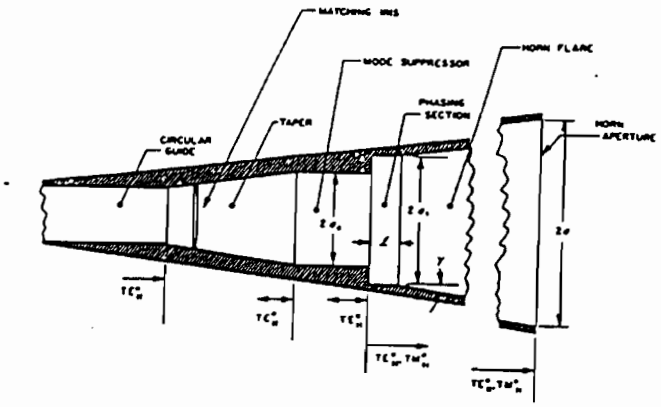

FIGURE I The Potter horn

the projected aperture of the antenna. These results are then used to derive expressions for the gain and the beam efficiency of the antenna and to calculate the co-polar and cross-polar antenna radiation patterns. In particular, we investigate the useful bandwidth of the antenna for high performance SIS split-block mixers. This will allow us to incorporate a high performance and yet easy-to-machine horn into our split-block technology, one which we have been developing over the past few years.

THE POTTER HORN

The conventional Potter Horn

The idea of synthesising a field distribution over the aperture of a horn by combining orthogonal waveguide modes was first suggested and successfully implemented by Potter (Potter, 1963). Potter demonstrated that a dual-mode horn could be realised by exciting both the TE_{11} and the TM_{11} modes at the throat of the horn. He showed that the radiation pattern of the horn becomes circular if the two modes reach the horn aperture with a particular relative amplitude and phase. This means that the horn beamwidth becomes independent of polarisation and the sidelobes become low in both the E-plane and H-plane. By converting a small percentage of the incident power carried by the TE_{11} mode into the TM_{11} mode, the E-plane sidelobes cancel. This results in an E-plane beam pattern which is almost identical to the H-plane pattern which in itself is unaffected by the step discontinuity. Potter presented a detailed empirical procedure for designing dual-mode horns shown in Fig. 1. First, the TE_{11} and TM_{11} modes are launched at the step discontinuity with a relative amplitude α and relative phase . The two modes are then allowed to propagate in a straight circular waveguide section. As the modes propagate, the phase difference between the modes is reduced prior to being launched into the conical horn of semi-flare angle θ_o. The length of the phasing section is chosen so that the TE_{11} and TM_{11} modes are in phase at the horn aperture. It is this requirement of zero phase difference between modes at the horn aperture that limits the horn bandwidth. As an example, if we require the cross-polar level to be less then -20 dB, we find that horn has a bandwidth of 10%. The bandwidth increases to

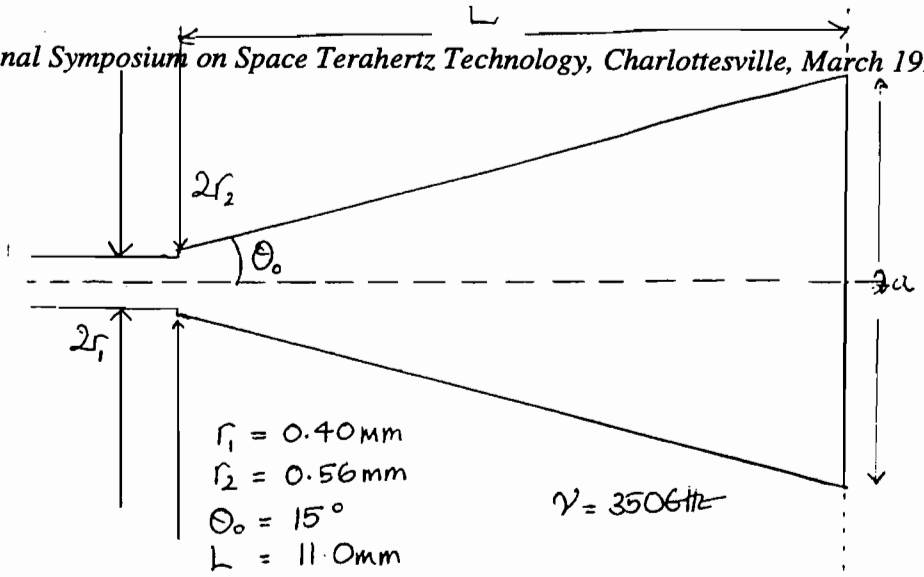

FIGURE II The Pickett-Potter horn

20% if the tolerance on the cross-polar level is relaxed to -16dB.

The Pickett-Potter horn

A simplified version of the conventional Potter horn was first introduced by Pickett *et. al* (Pickett, Hardy and Farhoomand, 1984). Here, the phasing section is removed, leaving a single step discontinuity at the throat of the horn (see Fig. 2). This simplifies greatly the horn fabrication, however, the relative phase between the modes can now only change as the modes propagate along the horn itself. As a result, the horn dimensions, normally chosen to obtain a predetermined beam shape, are now constrained by the requirements of minimum phase difference between the two modes. We shall show later that this in turn restricts the minimum allowed semi-flare angle and thus tends to increase the length of the horn. In all other respects, the electrical properties of this simplified horn should be identical to the original Potter horn.

Calculation of the electrical properties of the Pickett-Potter horn

We have calculated the field distribution across the aperture of the Potter horn using the well-known modal matching method. To do this, the horn is divided into discrete sections. At each junction a scattering matrix is calculated by matching the expansion coefficients of the field on either side of the junction and applying the constraint of conservation of power. The overall scattering matrix of the horn is calculated by cascading the matrices of the individual sections. In particular, the scattering matrix of the horn contains information about the complex mode coefficients across the horn aperture and the reflection coefficient at the horn input. Once the field distribution across the field aperture has been found, the radiation pattern of the horn can easily be calculated.

We have developed software to analyse the behaviour of the Pickett-Potter horn to be used for SIS mixer applications. The following parameters were used to define the horn: a centre frequency of 350 GHz, a semi-flare angle at 15° and an aperture diameter of a few millimetres. To simplify the calculation procedure, in particular for the horn-reflector antenna, we calculated the radiation pattern of the Pickett-Potter horn by assuming that the field at the aperture is given by that of a cylindrical waveguide, multiplied by the spherical phase error factor,

$\exp -j\frac{kr^2}{2L}$, where r is the radial distance in the horn aperture, k is the free space wavenumber and L is the horn length. The phase difference between the two modes as they propagate along the horn is given by

$$\Delta\phi = \int \frac{dz}{\lambda_{gTE}(z)} - \frac{dz}{\lambda_{gTM}(z)} \tag{1}$$

where z is axial distance along the horn. We have used this method in the past to calculate the radiation pattern of a corrugated horns and have obtained agreement between the computed and measured results down to -40 dB. Using Kirchhoff's aperture diffraction theory to calculate the radiated far fields we obtain:

$$E_\theta = \frac{jk\exp -jkR}{4\pi R}(1+\frac{\beta\cos\theta}{k})[f_x\cos\phi + f_y\sin\phi] \tag{2}$$

$$E_\phi = -\frac{jk\exp -jkR}{4\pi R}(\cos\theta+\frac{\beta}{k})[f_x\sin\phi - f_y\cos\phi] \tag{3}$$

where R,θ and ϕ are the spherical coordinates of the plane of observation, β is the guided propagation constant and $f_{x,y}$ are the far field components of the $E_{ax,y}$ aperture field components and can be written as:

$$\underline{\mathbf{f}} = \int_0^{2\pi}\int_0^a \underline{\mathbf{Ea}}(r',\phi')\exp[jkr'\sin\theta\cos(\phi-\phi')]r'dr'd\phi' \tag{4}$$

The co-polar and cross-polar patterns can then be written using Ludwig's third definition of cross polarisation as:

$$\begin{pmatrix} E_{cp} \\ E_{xp} \end{pmatrix} = \begin{pmatrix} \sin\theta & \cos\phi \\ \cos\theta & -\sin\phi \end{pmatrix}\begin{pmatrix} E_\theta \\ E_\phi \end{pmatrix} \tag{5}$$

An example of these calculations is shown in Fig. 3 where we have computed the radiation pattern at three frequencies. Note that the pattern quality at the optimum frequency (350 GHz) is comparable to that of a corrugated horn. By 380 GHz, however, the cross-polarisation level has already increased to -15 dB. A plot of the -3 dB and -10 dB beamwidths of the Pickett-Potter horn as a function of frequency is shown in Fig. 4. The best indicator of the bandwidth of the Pickett-Potter horn is the cross-polarisation level,(the sidelobe level is low over a very wide band). We have therefore plotted the cross-polar level as a function of frequency in Fig. 5, where the horn dimensions have been chosen to match those used in Fig. 3. We see that, over this frequency range, the cross polarisation level is comparable to that of a corrugated horn of similar dimensions and, unsurprisingly, much better than that of a diagonal horn over much of the frequency band of comparison.

A very useful design tool is the plot of the relative beamwidth of the horn ($\frac{\Delta\theta}{\theta_\circ}$) as a function of the phase error parameter Δ which defined as

$$\Delta = \frac{a}{\lambda}\tan\frac{\theta_\circ}{2} \tag{6}$$

An example design curve, which was computed for a fixed semiflare angle of 15° is given in Fig. 6.

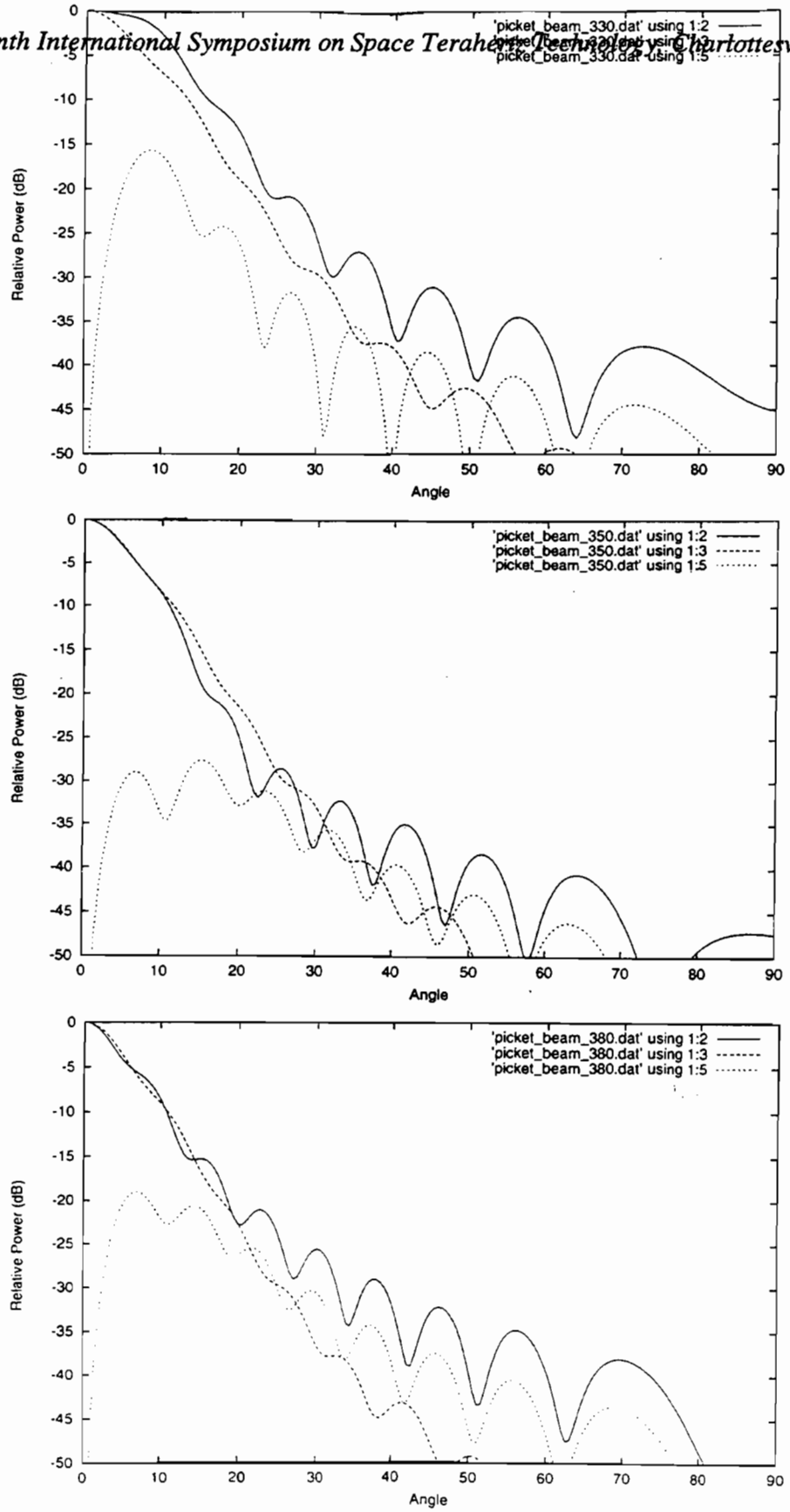

FIGURE III Pickett potter horn radiation patterns over the frequency range 330-380 GHz for a horn with semi-flare angle of 15° and length 11.6 mm . (a) 330 GHz (b) 350 GHz (c) 380 GHz.

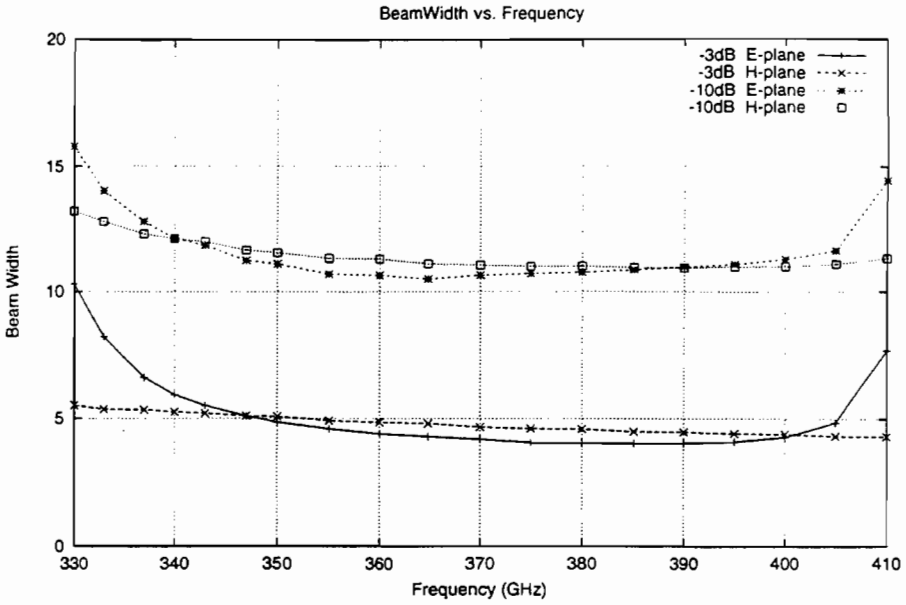

FIGURE IV -3 dB and -10 dB widths of the Potter horn

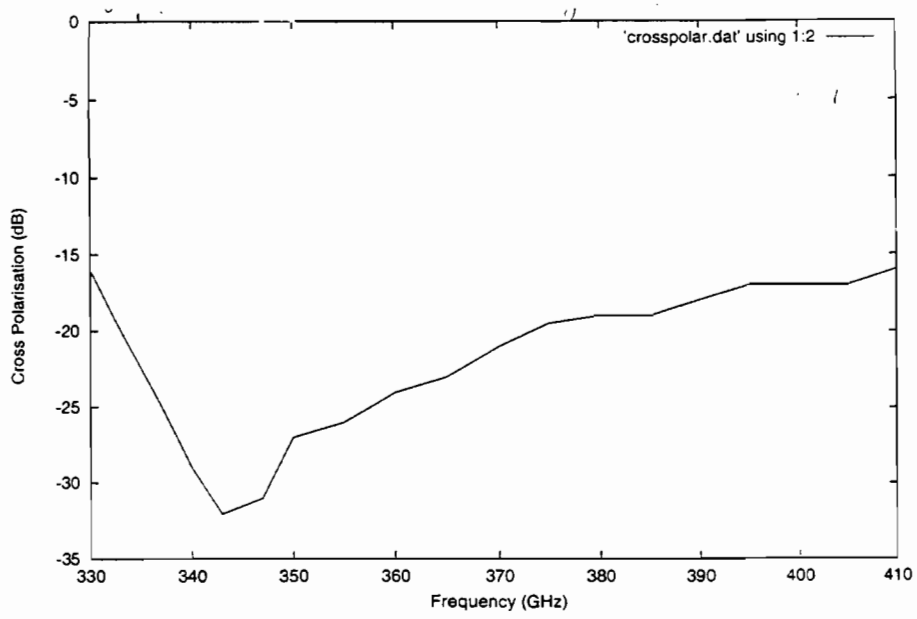

FIGURE V Cross polarisation level as a function of frequency for the Potter horn in Fig. 3

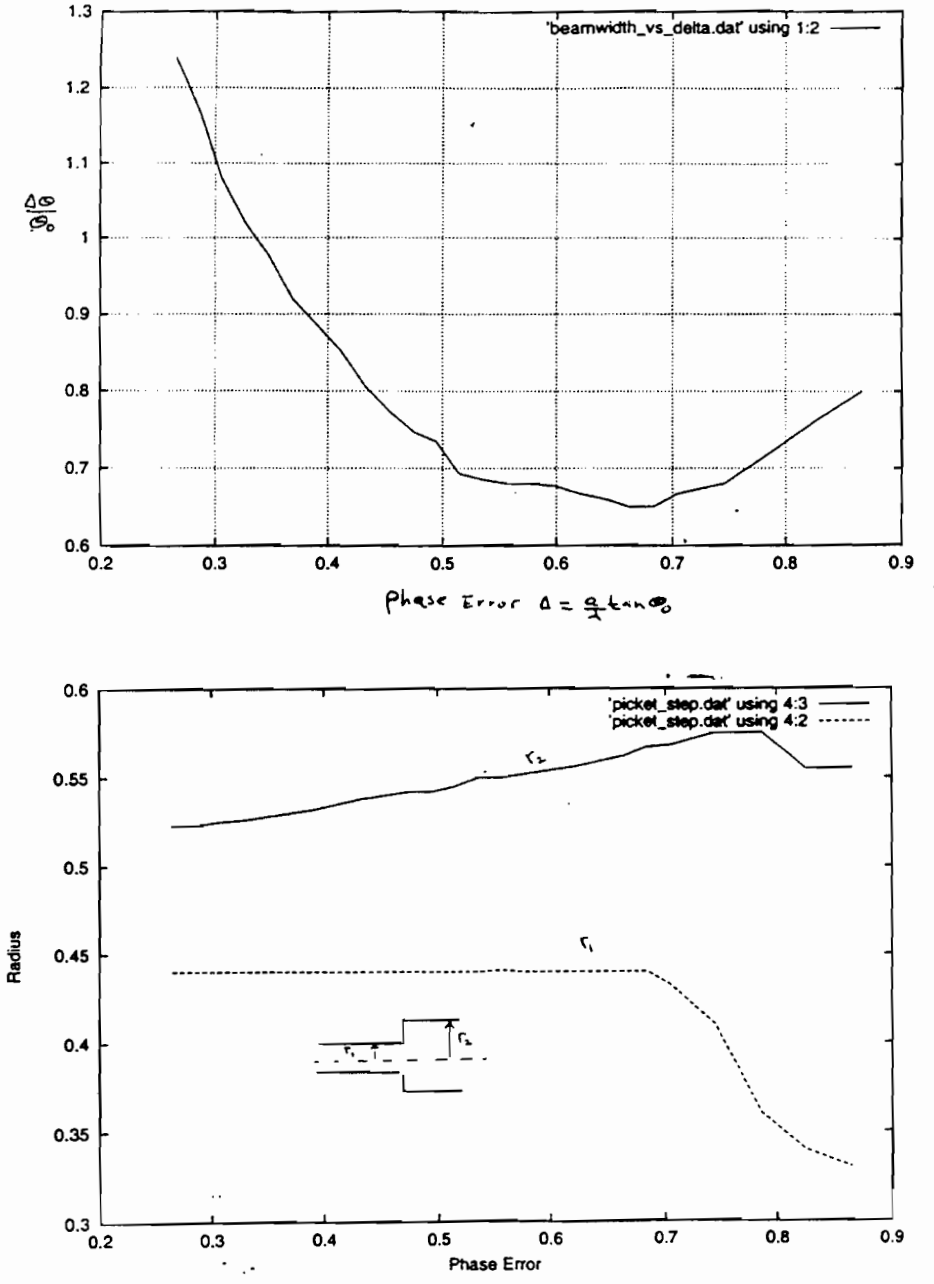

FIGURE VI A plot of the beamwidth of the Pickett-Potter horn as a function of the phase error, Δ, as defined by eqn. 6. The semi-flare angle of the horn was fixed at 15°

It should be noted that at each point on the plot the dimensions of the step were adjusted (by varying r_1, r_2) to give optimum performance (minimum cross-polarisation). It is interesting to note that the plot has a minimum which corresponds to the minimum beamwidth for a given horn semi-flare angle. A similar minimum occurs for corrugated horns, where the horn design becomes "optimum" in the sense of having maximum gain. Less encouraging was the discovery that the dynamic design range is severely compromised by the absence of the phasing section. This is why the phase error parameter cannot be increased to the values obtained by corrugated horns. In spite of this, it can be seen from Fig. 6 that a Pickett-Potter horn that is not diffraction-limited can still be realised using a moderately small flare angle.

THE POTTER HORN-REFLECTOR ANTENNA

Beams shape

The radiation pattern of a horn-reflector antenna fed by a conical horn is calculated by assuming that the parabolic reflector removes the spherical error of the horn. It is therefore assumed that the fields mapped onto the projected aperture are those of a cylindrical waveguide. This implies that an optimised horn design would automatically yield a good horn-reflector antenna pattern. This is because if the two modes reach the horn aperture in phase, then, assuming that the reflector only removes the quadratic phase error, they will also be in phase at the projected aperture plane. It should, however, be emphasised that if the length of the horn is changed, for example, to obtain a different beamwidth, then the step dimensions will also have to be changed in order to re-phase the two modes. Our analysis nevertheless shows that it is indeed feasible to realise a horn-reflector fed by a Pickett-Potter horn with performance comparable to that of a corrugated horn-reflector, however, a longer horn is required. This is demonstrated in Fig. 7 where we plotted the radiation pattern of the Potter horn-reflector antenna at two different frequencies. The patterns were computed for longitudinal input polarisation for either longitudinal (LL)or transverse (LT)observation planes (Yassin *et al*, 1993). It can be seen that the bandwidth of the antenna is at least as good as that of the horn and that the main beam shape resemble that of a corrugated horn. . In Fig. 8 we compare the pattern of a horn-reflector antenna fed by a Potter horn with those when the antenna is fed by either a corrugated horn or a smooth-wall conical horn. We notice that the sidelobes of the Potter antenna are comparable to those of the corrugated horn and are much lower than those obtained in the E-plane of the smooth wall conical horn. Finally, we would like to emphasise that in spite of the difficulties that arise from the phase error removal discussed above, the circularity of the Potter horn-reflector beam is insensitive to changes in the horn length. Apart from the expected change in beamwidth, the difference between the LL and LT main beams is very small as the length of the horn is increased from 2 cm to 6 cm. This can easily be understood by noting that the additional phase created at the aperture of the horn is a combination of the spherical phase error and the phase deference which results from the difference in the propagation constants of the TE_{11} and the TM_{11} modes. When the length of the horn is further increased the phase error change is removed, as usual, by the reflector and the

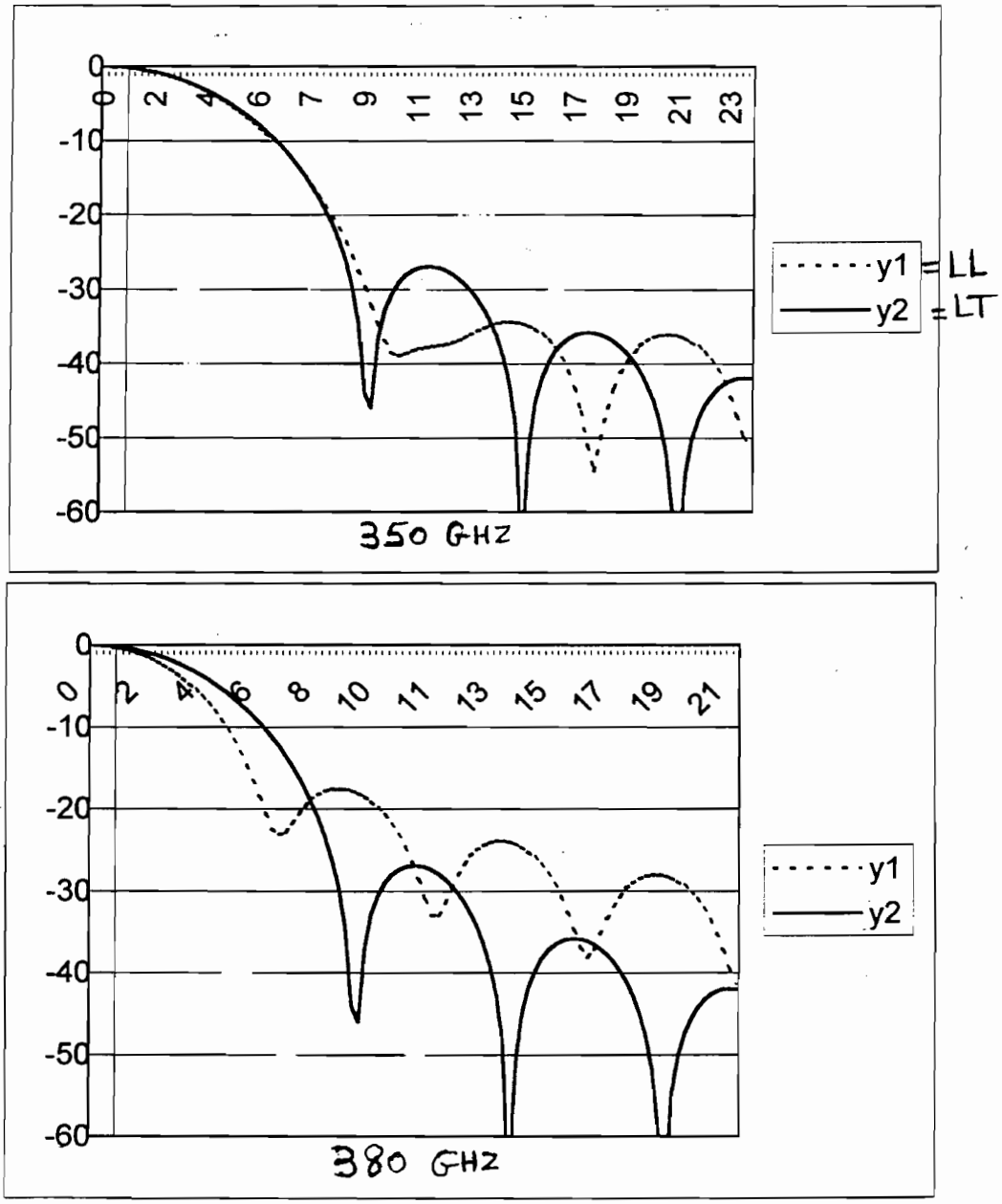

FIGURE VII Radiation patterns of the Potter horn-reflector antenna in the frequency range 330-380 GHz for a horn with semiflare angle of 15° and horn length of 1.65 cm for longitudinal polarisation. (a) 350 GHz (b) 380 GHz .

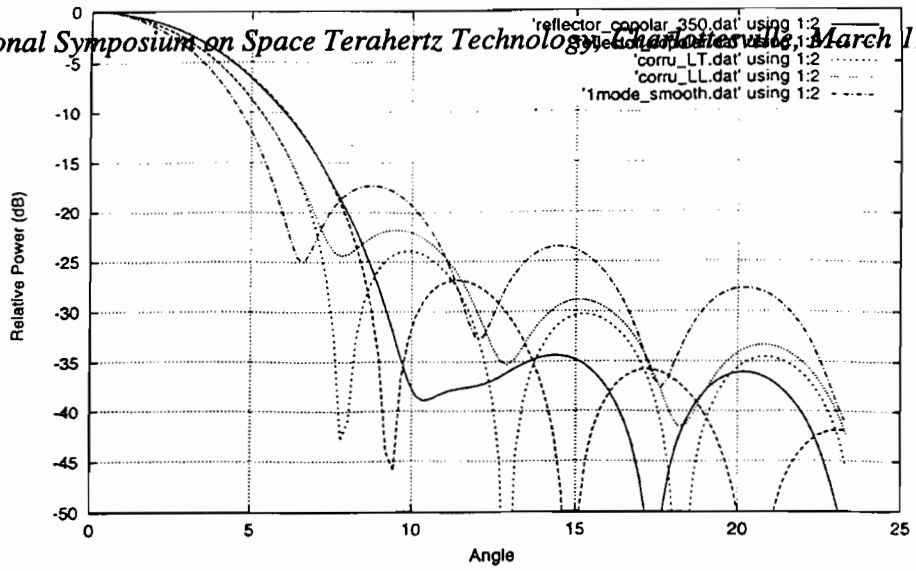

FIGURE VIII Comparison of the radiation patterns of the Potter horn-reflector antenna with those of corrugated and smooth wall conical horns.

change resulting from the difference in the propagation constant is very small. As a result, the phase change in the projected aperture remains very small and consequently the beam circularity is maintained. In contrast, the diameter of the projected aperture. which in fact determines the beamwidth, is proportional to the horn diameter, hence the beamwidth is substantially changed.

Design recipe

The procedure to design a Pickett-Potter horn-reflector antenna is similar to that would be used to design a corrugated horn-reflector. The following approximate design formulas are provided for the reader's convenience. The relation between the projected aperture diameter D and the full beamwidth is, for moderate semi-flare horn angles, is given by:

$$\Delta\theta \approx 1.2\frac{\lambda}{D} \tag{7}$$

The design of the horn reflector antenna can be realised as follows:

- Determine the diameter of the projected aperture according to the required beamwidth from the above formula
- Calculate the horn aperture diameter, d, according to the relation:

$$D = d[\frac{1+\sin\theta_o}{\cos\theta_o}] \tag{8}$$

- Design a potter horn with a semiflare angle $10° - 20°$ with optimum performance around the band centre frequency.
- Determine the focal length of the 90° offset parabolic reflector using the relation

$$D = 4f\tan\theta_o \tag{9}$$

- Calculate the radiation patterns of the antenna and refine the step discontinuity dimensions to achieve maximum beam circularity.

CONCLUSION

We have shown that the Pickett-Potter horn can be employed in conjunction with horn-reflector antennas, provided that the TE_{11} and TM_{11} modes reach the projected aperture in phase. Although the absence of a phasing section in the Picket-Potter version restricts the horn design flexibility, our study showed that practical horn-reflector antenna dimensions suitable for submillimetre-wave array receivers can still be found. The bandwidth of the antenna is clearly dependent on the specified cross- polarisation level. For example, a -20 db cross-polar level can be maintained over a fractional bandwidth of 10%, while -15 db level can be achieved over a fractional bandwidth of 25 %.

REFERENCES

Withington, S., Yassin, G., Buffey, M. and Norden, C. (1997): "A Horn-Reflector antenna for high performance submillimetre imaging arrays," *Int'l J. IR and MM Waves*, vol. 18, no. 2, pp. 341-358, 1997.

Potter, P. D. "A new horn antenna with suppressed sidelobes and equal beamwidths," *Microwave J.*, **6** pp. 71-78, 1963. finline mixer for astronomical imaging arrays ," Elctron. Lett. Vol. 33, PP. 498–500, 1997.

Pickett, H. M., Hardy, J. C. and Farhoomand, J., "Characterisation of a dual-mode horn for submillimetre wavelengths," *IEEE Trans. Microwave Theory Tech.* MTT–32, no. 8, pp. 936-937, 1984.

Silver, S. *Microwave antenna theory and Design*, McGraw-Hill Book Co., Inc., New York, 1949, pp. 162.

Yassin, G., Robson, M. and Duffett–Smith, P. J. "The electrical characteristics of a conical horn–reflector antenna employing a corrugated horn", *IEEE Antennas and propagation*, vol. AP-41, pp. 357–361, April 1993.